ChemComm

Accepted Manuscript

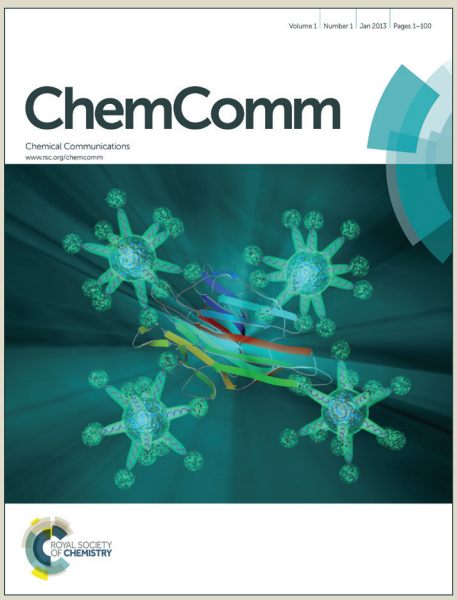

ROYAL SOCIETY OF CHEMISTRY

www.rsc.org/chemcomm

Cite this: DOI: 10.1039/c0xx00000x

www.rsc.org/xxxxxx

ARTICLE TYPE

Conformational Change and Biocatalysis-Triggered Spectral Shift of Single Au Nanoparticles

Yun Zhao, Ya-Kai He, Jing Zhang, Feng-Bin Wang, Kang Wang*, Xing-Hua Xia*

Spectral shift of localized plasmon resonance scattering of guanine-rich DNA modified single Au nanoparticles are observed under dark field microscopy equipped with a spectrometer. The spectra continuously red-shift with the conformational change of the guanine-rich DNA upon associating with K^+, hemin and the biocatalytic growth of polymer. The scattering spectrum of single nanoparticle is proved to be sensitive both to subtle conformational change and biocatalysis process. 20 mM K^+ or 100 μM H_2O_2 can trigger a detectable peak shift. The present study paves a new and efficient way to extract chemical information from micro/nano space.

Plenty of essential biological phenomena, such as DNAzyme-involved gene replication and ribozyme-involved protein synthesis, are accompanied with the conformational change and biocatalysis process of biomolecules. For instance, folding of telomeric DNA into G-quartet structures inhibits its use by telomerase, thus influencing the extent of telomere elongation inside cancer cells.[1] Hence, developing methods to detect these processes is fundamentally important for life study. Various kinds of methods including fluorescence,[2,3,4] electrochemistry,[5,6,7] atomic force microscopy[8,9] and localized surface plasmon resonance[10,11,12] (LSPR) have been applied for monitoring biomolecular binding events.

LSPR of single nanoparticles, also known as nanoparticle plasmon resonance (NPPR), is of growing interests since it provides a direct pathway for tracking bioprocesses in micro/nano space. NPPR is a phenomenon that the electrons in metal nanoparticles collectively resonate with the incident light during which the excited oscillation is spatially confined within the physical boundary of nanoparticles. The resonance frequency can be modulated by biomolecule induced metal growth[13] and variation of environmental dielectric constant.[14,15] Compared with fluorescence, NPPR is sensitive to the change of local nanoenvironment without concerning about those conventional adventures of photo-bleaching and single molecule intensity fluctuations (i.e. blinking), which makes it a promising nanoprobe for biosensing.[16,17,18,19]

Development of stimuli-responsive plasmonic resonant nanoparticles is the key issue for single-molecule sensing and imaging. Pioneer works on the probing of biological processes on metal nanostructures and metal nanoparticles have been conducted by several research groups. Van Duyne group demonstrated a calcium-modulated plasmonic switch based on the calcium-induced conformational changes of calmodulin by measuring the extinction maximum of nanostructured surface plasmon resonance.[11] Liphardt group constructed a molecular ruler based on plasmon coupling of single gold and silver nanoparticles to study the kinetics of DNA hybridization event.[20] Lee group first reported the phenomenon of plasmon resonance energy transfer (PRET) on a single Au nanoparticle upon adsorption of cytochrome c.[21] Wealso constructed a pH sensitive nano-assembly based on i-motif DNA linked Au nanoparticles.[22] Very recently, Rajesh group demonstrated a light-induced photo-reversible molecular machine to detect the photoisomerization of azobenzene molecules in solid state.[23] For further application of single nanoparticles in bioanalysis, understanding the effect of conformational change and biocatalysis processes on the NPPR character of single nanoparticle is of significant importance.

Herein, we demonstrate spectral shift of single gold nanoparticles (GNPs) triggered by the association process of guanine-rich DNA sequence (G-DNA) with K^+ and hemin. Scheme 1 illustrates the conformational change and biocatalysis process of G-DNA on a single GNP. Briefly speaking, G-DNA was first conjugated to GNP via thiol-Au bond (a). Upon addition of K^+, the guanine-rich DNA folded into a quadruplex structure (b). Further association of G-quadruplex with hemin formed DNAzyme (c) which can catalyse the oxidation of DAB in presence of hydrogen peroxide and form precipitate around the surface of GNP (d). Experimental results show that subtle variation, including the conformational change of G-DNA, can be detected through recording the scattering spectra of the single GNPs. Subsequent reaction catalyzed by the G-DNA-K^+-hemin complex also indicates that NPPR can be directly used in sensing bioactive small molecules, such as hydrogen peroxide, in micro/nano space.

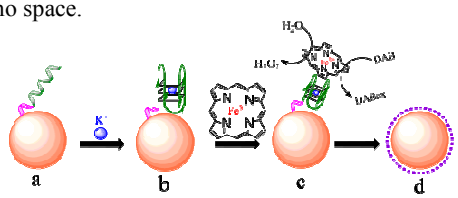

Scheme 1. Illustration of the conformational change and biocatalysis process of G-DNA-modified GNP.

The details for DNA preparation and the instrument used are described in Supporting Information.

The DNA sequences used in the experiment were as follows:

5'-TTTTTTGGGTAGGGCGGGTTGGGTTTTTT-S-S-3'(G-DNA,extinction coefficient = 265700 L·mole-1cm-1)

5'-AGCCTGATGTCGTCATAACTGA-(CH2)3-S-S-3'(R-DNA, extinction coefficient = 215900 $L \cdot mole^{-1}cm^{-1}$)

The GNPs were modified on glass slides using a novel method based on electrostatic adsorption. The details are described in Supporting Information.

All the attachment chemistry was conducted on the exposing surface of GNPs modified on glass slide which was covered by a piece of PDMS with an 8 mm hole serving as the sample cell. The chamber had a volume of approximate 80 μL. G-DNA was dissolved in 1 M KCl buffer with a final concentration of 2 μM. For a typical experiment, an 80 μL DNA stock solution was dropped into the chamber. After two hour incubation, the chamber was carefully rinsed with deionized water to remove any non-specifically adsorbed DNA chains.

The dark-field measurements were carried out on an inverted microscope equipped with a dark-field condenser (0.8 <NA<0.95) and a 60Xobjective lens (NA=0.7). Typically, about 80μL different kinds of buffer (1 M KCl, deionized water or 10 mM Tris-HCl buffer with 500 mM KCl) were dropped into the chamber on the slides. The dark-field images of GNPs were collected by a colored CCD. The scattering spectra of the GNPs were obtained by switching the light path into a spectrograph equipped with a grating (grating density: 300 lines/mm; blazed wavelength: 600 nm).

Kinetics was followed by measuring the NPPR scattering spectra of the oligonucleotide-modified GNPs with designated time interval. Typically, 60 μL buffer (10 mM Tris-HCl + 500 mM KCl) was dropped into the reaction chamber after a previous immersion of the chamber in 500 nM hemin solution. Then, DAB and H_2O_2 stock solution were added with a final concentration of 0.1 mM DAB and 100 μM H_2O_2, respectively.

In the first step, dark field images were obtained to locate the single GNPs immobilized on the glass slide. Then, the scattering spectra of selected GNPs were recorded. Figure 1a illustrates the light path configuration for imaging and spectrum recording. As shown in Figure 1b, GNPs of 50 nm-diameter distribute randomly on the glass slide with intrinsic green scattering light. Individual yellow to red spots occasionally appear in the image which may be caused by the slight aggregation during the immobilization process (Figure S1). Figure 1c shows the NPPR spectra of two spots labeled in Figure 1b. The band for the circle-labeled spot locates at 547 nm and the one for the square-labeled spot locates at 549 nm. A statistics of 21 spectra of green colored GNPs gives the peak position ranging from 537 to 557 nm (Figure S2), which is attributed to the size non-uniformity of different GNPs and their delicately different surface environments. Although the maximum peak of the initial GNPs distributes between 537 nm to 557 nm, the stability and reliability of each GNP is out of question. Control experiment shows that the maximum peak of each isolated GNP itself will not shift within several hours.

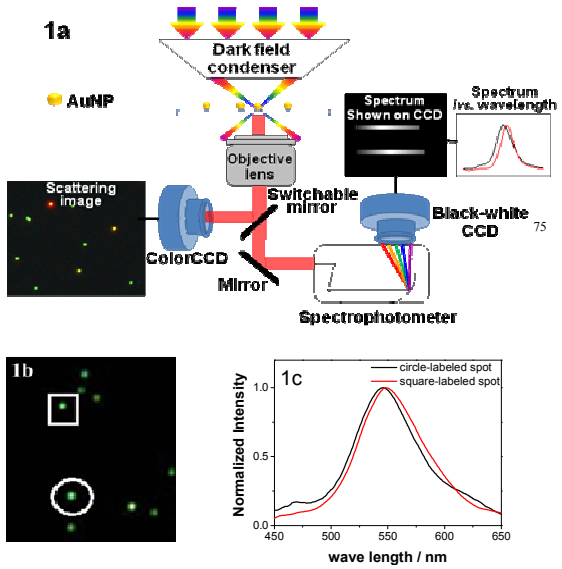

Figure 1. (a) Schematic diagram of the light path for imaging and spectrum recording. (b) Dark field image of surface immobilized GNPs. (c) NPPR scattering spectra of surface immobilized GNPs with different size.

After *in situ* immobilization of DNA on GNPs, the solution was changed back to deionized water to avoid forming any folding structure of G-DNA. Then we measured the NPPR scattering spectrum of the same GNP in response to different stimuli. As demonstrated in Figure 2a, for a GNP with the NPPR spectrum peak (λ_{max}) centered at 546 nm, surface covalent binding of G-DNA makes the peak position red-shift to 548 nm. After the addition of KCl solution to the reaction chamber, the NPPR peak shifts to 550 nm, suggesting a subtle change occurs which affects the NPPR property of the GNPs. When 500 nM hemin presents in the solution, the NPPR peak further shifts to 555 nm. Because the GNPs were immobilized on the substrate stably, no GNP aggregation could occur during the experiment. Moreover, with the help of a slit and CCD, we can exactly focused on the same GNP each time and carried out all the measurements *in situ*, so the spectral fluctuation of GNPs themselves can also be excluded. Then, the continuous shift of the NPPR peak upon stimulation can be attributed to the change within the nanoenvironment surrounding the nanoparticles.

According to the Mie theory[24], NPPR spectrum character of an isolated metal nanosphere embedded in an external dielectric medium depends on the nanoparticle radius A, the dielectric function of nanoparticle (ε_i and ε_r, the imaginary and real portion of the metallic nanoparticle's dielectric function) and the nanoenvironment's dielectric constant (ε_m). Kathryn[25] simplified the functional form as following:

$$\lambda_{\max} = \lambda_p \sqrt{2\varepsilon_m + 1} = \lambda_p \sqrt{2n_m^{\,2} + 1} \qquad (1)$$

where λ_{max} is the wavelength of NPPR peak, λ_p is the wavelength corresponding to the plasma frequency of the bulk metal and n_m is the refractive index. For the present study, surface immobilization of G-DNA increases the surface charge density, thus causing a direct change in the dielectric constant within the nanoenvironment around the metal nanoparticles. It is acknowledged that G-rich DNA will fold into a quadruplex configuration in the presence of certain monovalent ions, especially potassium. Circular dichroism measurement of the G-DNA in bulk solution (Figure S3) gives a positive peak at 269 nm and a negative peak at 239 nm, respectively, indicating the formation of a parallel G-quadruplex structure in the presence of 20 mM KCl.[26] The compact size of the folded G-DNA is about 2.2 nm[27]. Given that the length of G-DNA we used is approximately 9.9 nm in length, the folding of G-DNA will only cause a 3.6 nm decrease in the distance between G-DNA layer and GNP. Such a slight change will lead to a very small change in the dielectric constant around GNPs. Therefore, the NPPR peak red shifts for only about 2 nm upon the formation of G-quadruplex (Figure 2a, blue curve). The experimental results are consistent to the previous study on a plasmonic ruler[20], in which the hybridization of DNAs caused a 2 nm change in DNA chain length, leading to ~2 nm NPPR spectral shift.

More interestingly, when switching the solution back and forth between pure water and Tris-HCl buffer with 500 mM K^+, a reversible spectral shift was observed (Figure 2b). The phenomenon indicates that the conformational change of G-DNA upon association with K^+ is a reversible process and the scattering spectrum of a single nanoparticle is highly sensitive to the conformational change of the small amount of surface-attached molecules.

Further binding of G-quadruplex with hemin molecule brings an obvious increase of the refractive index around GNPs, leading to a larger red-shift of the NPPR peak. It is worthy to note that similar red-shift of NPPR scattering peak can always be observed regardless of the initial peak position of the GNPs, indicating the good reproducibility and reliability of such detecting method. The spectral shifts of single GNPs with different initial peak positions are shown in Figure S4.

For comparison, a random DNA sequence (R-DNA) is immobilized on the GNPs instead of G-DNA (Figure S5). No peak shift is observed after adding KCl to the solution, showing a constant configuration of the R-DNA. Further introduction of hemin also leads to no obvious peak shift. These observations support the above deduction that the red-shift of NPPR peaks in Figure 2a is caused by the conformational change of G-DNA and the further combination of hemin with the G-quadruplex.

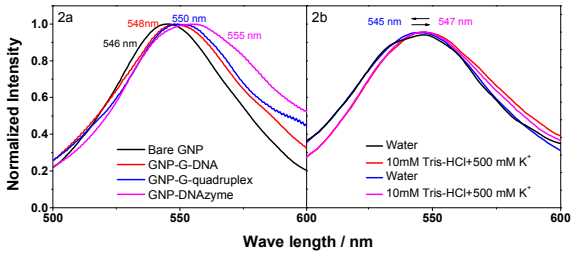

Figure 2. (a)The NPPR scattering spectra of the G-DNA-modified GNP. (b) The reversible spectra shift of the G-DNA-modified GNP upon adding/removing K^+.

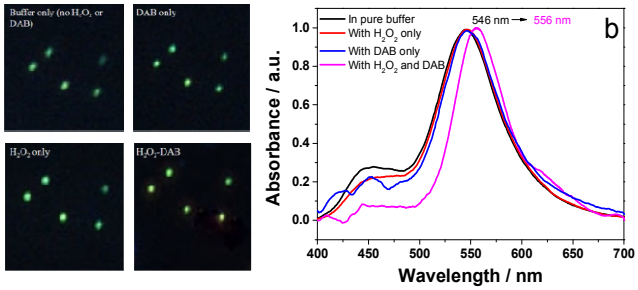

Figure 3.(a) DFM images of GNP-DNAzyme in the presence of different solutions. (b) The scattering spectra shift of a GNP-DNAzyme in different solutions. H_2O_2: 100 μM, DAB: 0.1 mM

As biocatalysis reactions play important roles in life processes, we tested the catalytic behavior of single particle toward H_2O_2. G-quadruplex-hemin is known as a horseradish peroxidase (HRP) mimicking DNAzyme which can catalyseH_2O_2-mediated oxidation of benzidine (DAB).[28] Figure 3a shows the DFM images of GNP-G-quadruplex-hemin (GNP-DNAzyme) in the presence of different solutions. Each spot in the DFM photos represents a single GNP. When only DAB or H_2O_2 presents in the solution, the colour of GNPs shows no change from the one recorded in pure buffer. The corresponding NPPR scattering spectra (Figure 3b) also shows no peak shift. When both H_2O_2 and DAB present in the solution, a subtle colour change occurs. Correspondingly, the scattering peak shows a red-shift of 10 nm within 55 min.

The change of scattering spectra of GNP-DNAzyme with time was also studied. As shown in Figure 4, the scattering peak continuous red-shift after the addition of 100 μM H_2O_2 in the presence of 0.1mM DAB. The corresponding red-shifting of λ_{max} with time is plotted as the inset. It can be seen that, for the GNP under observation, the peak-shift increase up to approximate 9 nm within 55 min, and then approaches to a stable state. Moreover, when the hemin-attached G-DNA was substituted by a random DNA which also undergoes the hemin treatment step, no NPPR peak shift was observed even in the presence of H_2O_2-DAB solution (Figure S6). The above observations suggest that the peak shift in Figure 3b is caused by the oxidation of DAB by H_2O_2. Since the oxidation product of DAB is a brown precipitate and the surface immobilized DNAzyme only catalyzes the oxidation reaction around GNPs, it will bring an adsorbate-induced refractive index change on the plasmonic GNPs.

For different GNPs in the same solution or in the solution with higher H_2O_2 concentration, such peaks all show a red-shift but the extent of shifting varies from case to case (Figure S7). In order to better clarify the good reproducibility, we concluded

several sets of experiment data into two tables. Table 1 features the NPPR shift upon the DNA conformation change and Table 2 exhibits the NPPR shift during the biocatalytic process. As indicates from both Tables, all GNPs present a similar NPPR shift in spite of the different initial location of its peak wavelength. These results reflect the good reproducibility and reliability of the present method. Moreover, the kinetic curves of the peak shift (insets of Figure 4 and Figure S7) usually give two plateaus which may correspond to the adsorption of DAB on the GNP-DNAzyme and the DNAzyme-catalyzed oxidation and polymerization of DAB, respectively. Further study of the formation of these two plateaus is undergoing. However, the tendency that all the peak shifts eventually reach a saturated state indicates that the GNP-DNAzyme catalyzed reaction is self-confined around the nanoparticle, which makes the NPPR scattering spectrum a promising tool for detecting catalytic reactions in micro/nano space.

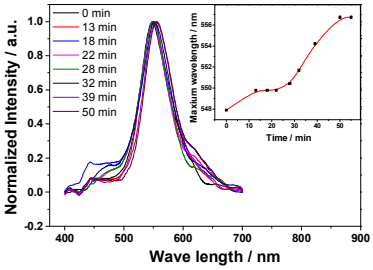

Figure 4. The NPPR scattering spectra of the immobilized GNP-DNAzyme in 0.1 mM DAB and 100 μM H_2O_2 solution.

Table 1. NPPR peak wavelength during G-DNA conformational change on different GNPs.

	NPPR peak Wavelength / nm							
GNP-G-DNA	541	546	547	548	549	558	562	566
GNP-G-quadruplex	543	548	549	550	550	559	563	568
GNP-DNAzyme	548	554	554	555	555	563	567	573

Table 2. NPPR wavelength shift during biocatalytic process toward H_2O_2-DAB on different GNPs.

	Spot 1	*Spot 2*	*Spot 3*	*Spot 4*	*Spot 5*
Δ λ /nm	9	9	8	8	10

Through the combination of NPPR and dark field imaging technology, we achieve the direct observation of conformational change of G-rich DNA from a random coil structure to a parallel G-quadruplex one on single gold nanoparticle. The specific molecule recognition event of hemin to G-quadruplex further amplifies the NPPR shift. The formed GNP-DNAzyme exhibits localized catalytic response toward H_2O_2-DAB and therefore can be used as a potential nanoprobe for the detection of H_2O_2 in micro/nano space. More significantly, by substituting the G-DNAs with other specified oligonucleotide sequence, versatile nanoporbes can be made for various kinds of bioanalysis.

This work was supported by the grants from the National 973 Basic Research Program (2012CB933800), the National Natural Science Foundation of China (21327902, 21035002, 21275070, 21275071, 21205059), the National Science Fund for Creative Research Groups (21121091), and the Program for New Century Excellent Talents in University (NCET-11-0237).

State Key Laboratory of Analytical Chemistry for Life Science, School of Chemistry and Chemical Engineering, Nanjing University, Nanjing 210093, China. Fax: +86-25-83685947; Tel: +86-25-83597436; E-mail: wangkang@nju.edu.cn (K. Wang); xhxia@nju.edu.cn(X.H. Xia)

References

(1)Zahler, A. M.; Williamson, J. R.; Cech, T. R.; Prescott, D. M. *Nature.***1991**, *350*, 718.
(2)Kim, E.; Lee, S.; Jeon, A.; Choi, J. M.; Lee, H. S.; Hohng, S.; Kim, H. S. *Nat. Chem. Biol.***2013**, *9*, 313.
(3)Sajadi, M.; Furse, K. E.; Zhang, X.X.; Dehmel, L.; Kovalenko, S. A.; Corcelli, S. A.; Ernsting, N. P. *Angew. Chem. Int. Ed.***2011**, *50*, 9501.
(4)He, S.; Song, B.; Li, D.; Zhu, C.; Qi, W.; Wen, Y.; Wang, L.; Song, S.; Fang, H.; Fan, C. *Adv. Funct. Mater.* **2010**, *20*, 453.
(5)Lubin, A. A.; Plaxco, K. W. *Acc. Chem. Res.* **2010**, *43*, 496.
(6)Napier, M. E.; Loomis, C. R.; Sistare, M. F.; Kim, J.; Eckhardt, A. E.; Thorp, H. H. *Bioconjugate Chem.***1997**, *8*, 906.
(7)Calvo, E. J.; Battaglini, F.; Danilowicz, C.; Wolosiuk, A.; Otero, M. *Faraday Discuss.***2000**, *116*, 47.
(8)Kienberger, F.; Ebner, A.; Gruber, H. J.; Hinterdorfer, P. *Acc. Chem. Res.***2006**, *39*, 29.
(9)Bizzarri, A. R.; Cannistraro, S. *Chem. Soc. Rev.***2010**, *39*, 734.
(10)Hall, W. P.; Ngatia, S. N.; Van Duyne, R. P. *J. Phys. Chem. C* **2011**, *115*, 1410.
(11)Hall, W. P.; Anker, J. N.; Lin, Y.; Modica, J.; Mrksich, M.; Van Duyne, R. P. *J. Am. Chem. Soc.* **2008**, *130*, 5836.
(12)Guo, L.; Kim, D.H. *Biosens. Bioelectron.***2012**, *31*, 567.
(13)Zhang, L.; Li, Y.; Li, D.W.; Jing, C.; Chen, X.; Lv, M.; Huang, Q.; Long, Y.T.; Willner, I. *Angew. Chem. Int. Ed.***2011**, *50*, 6789.
(14)Miller, M. M.; Lazarides, A. A. *J. Phys. Chem. B.***2005**, *109*, 21556.
(15)Xu, G.; Chen, Y.; Tazawa, M.; Jin, P. *Appl. Phys. Lett.***2006**, *88*.
(16)Xiong, B.; Zhou, R.; Hao, J.; Jia, Y.; He, Y.; Yeung, E. S. *Nat. Commun.***2013**, *4*, 1708.
(17)Li, Y.; Jing, C.; Zhang, L.; Long, Y. T.*Chem. Soc. Rev.***2012**, *41*, 632.
(18)Susie, E.;Mostafa, A. E-S.*Chem. Soc. Rev.***2006**, *35*, 209.
(19) Shi, Le.; Jing, C.; Ma, W.; Li, D. W.; Halls, J. E.; Marken, F.; Long, Y. T. *Angew. Chem. Int. Ed.***2013**, 52, 6011.
(20)Sonnichsen, C.; Reinhard, B. M.; Liphardt, J.; Alivisatos, A. P. *Nat. Biotechnol.***2005**, *23*, 741.
(21)Liu, G. L.; Long, Y. T.; Choi, Y.; Kang, T.; Lee, L. P. *Nat. Methods* **2007**, *4*, 1015.
(22)Zhao, Y.; Cao, L.; Ouyang, J.; Wang, M.; Wang, K.; Xia, X.H. *Anal. Chem.***2013**, *85*, 1053.
(23)Joshi, G. K.; Blodgett, K. N.; Muhoberac, B. B.; Johnson, M. A.; Smith, K. A.; Sardar, R. *Nano Lett.* **2014**.
(24)Mie, G. *Ann.Phys.***1908**, *377*, 25.
(25)Mayer, K. M.; Hafner, J. H. *Chem. Rev.***2011**, *111*, 3828.
(26)Xue, Y.; Kan, Z. H.; Wang, Q.; Yao, Y.; Liu, J.; Hao, Y. H.; Tan, Z. *J. Am. Chem. Soc.* **2007**, *129*, 11185.
(27)Alberti, P.; Mergny, J. L. *Proc. Natl. Acad. Sci. U.S.A.***2003**, 100(4), 1569.
(28)Josephy, P. D.; Subden, R. E. *Mutat. Res.***1984**, *141*, 23.